Cell Reports

Phosphorylated EGFR Dimers Are Not Sufficient to Activate Ras

Graphical Abstract

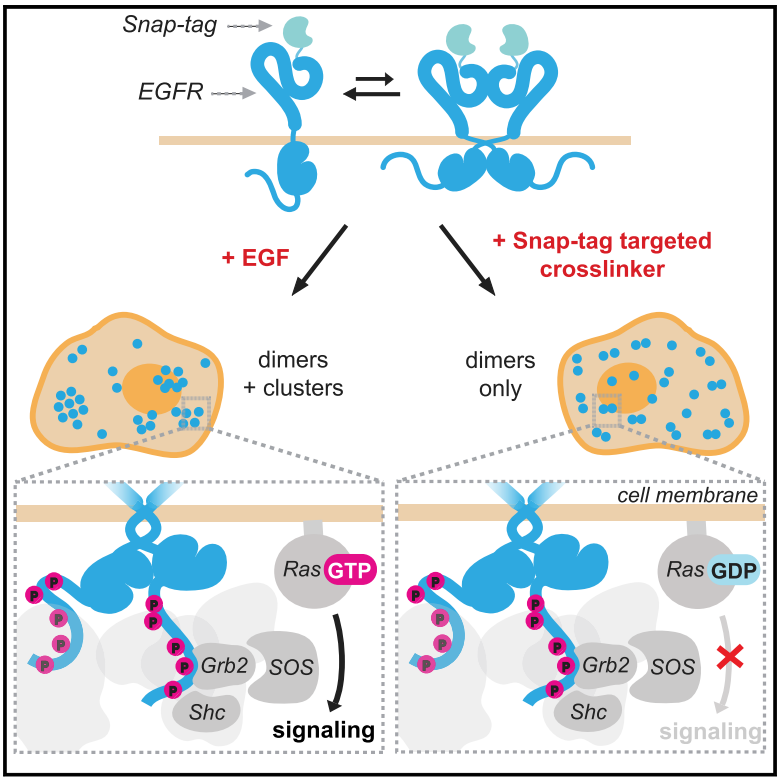

Authors

Samantha I. Liang, Bettina van Lengerich, Kelsie Eichel, ..., Mark von Zastrow, Natalia Jura, Zev J. Gartner

Correspondence

natalia.jura@ucsf.edu (N.J.), zev.gartner@ucsf.edu (Z.J.G.)

In Brief

Liang et al. demonstrate that the recruitment of key signaling adapters to stable phosphorylated EGFR dimers is not sufficient for the activation of Ras and its downstream pathways. Binding of EGFR ligands induces conformational changes and receptor dynamics necessary for oligomerization and efficient signal propagation through the SOS-Ras-MAPK pathway.

Highlights

- Chemical-genetic approach to form stable phosphorylated EGFR dimers on cells
- Chemically induced dimers recruit adaptors to a similar extent as EGF-activated EGFR
- SOS, Grb2, and Shc recruitment to EGFR dimers is not sufficient for Ras activation
- EGF induces conformational changes necessary for higher order oligomer formation

Liang et al., 2018, Cell Reports *22*, 2593–2600
March 6, 2018 © 2018 The Authors.
https://doi.org/10.1016/j.celrep.2018.02.031

CellPress

Cell Reports
Report

OPEN ACCESS
CellPress

Phosphorylated EGFR Dimers Are Not Sufficient to Activate Ras

Samantha I. Liang,[1,2] Bettina van Lengerich,[3] Kelsie Eichel,[2,5] Minkwon Cha,[8,9,10] David M. Patterson,[1] Tae-Young Yoon,[9,10,11] Mark von Zastrow,[4,5] Natalia Jura,[3,4,12,*] and Zev J. Gartner[1,6,7,12,13,*]
[1]Department of Pharmaceutical Chemistry, University of California, San Francisco, San Francisco, CA, USA
[2]Program in Biochemistry and Molecular Biology, University of California, San Francisco, San Francisco, CA, USA
[3]Cardiovascular Research Institute, University of California, San Francisco, San Francisco, CA, USA
[4]Department of Cellular and Molecular Pharmacology, University of California, San Francisco, San Francisco, CA, USA
[5]Department of Psychiatry, University of California, San Francisco, San Francisco, CA, USA
[6]Chan Zuckerberg Biohub, University of California, San Francisco, San Francisco, CA, USA
[7]Center for Cellular Construction, University of California, San Francisco, San Francisco, CA, USA
[8]Department of Physics, Korea Advanced Institute of Science and Technology (KAIST), Daejeon 34141, South Korea
[9]Center for Nanomedicine, Institute for Basic Science (IBS), Yonsei University, Seoul 30722, South Korea
[10]Yonsei-IBS Institute, Yonsei University, Seoul 30722, South Korea
[11]Department of Biological Sciences, Seoul National University, Seoul 08826, South Korea
[12]Senior author
[13]Lead Contact
*Correspondence: natalia.jura@ucsf.edu (N.J.), zev.gartner@ucsf.edu (Z.J.G.)
https://doi.org/10.1016/j.celrep.2018.02.031

SUMMARY

Growth factor binding to EGFR drives conformational changes that promote homodimerization and transphosphorylation, followed by adaptor recruitment, oligomerization, and signaling through Ras. Whether specific receptor conformations and oligomerization states are necessary for efficient activation of Ras is unclear. We therefore evaluated the sufficiency of a phosphorylated EGFR dimer to activate Ras without growth factor by developing a chemical-genetic strategy to crosslink and "trap" full-length EGFR homodimers on cells. Trapped dimers become phosphorylated and recruit adaptor proteins at stoichiometry equivalent to that of EGF-stimulated receptors. Surprisingly, these phosphorylated dimers do not activate Ras, Erk, or Akt. In the absence of EGF, phosphorylated dimers do not further oligomerize or reorganize on cell membranes. These results suggest that a phosphorylated EGFR dimer loaded with core signaling adapters is not sufficient to activate Ras and that EGFR ligands contribute to conformational changes or receptor dynamics necessary for oligomerization and efficient signal propagation through the SOS-Ras-MAPK pathway.

INTRODUCTION

Epidermal growth factor receptor (EGFR) is a broadly expressed receptor tyrosine kinase frequently mutated or overexpressed in cancer. The steps of EGFR activation by ligands such as EGF have been extensively studied. Biochemical, imaging, and structural evidence support a model wherein monomers of EGFR are inactive and in equilibrium with a population of inactive dimers (Chung et al., 2010; Jura et al., 2009). Binding of EGF stabilizes receptor conformations that expose an extracellular dimerization interface, triggering accumulation of active EGFR dimers (Ferguson et al., 2003; Ogiso et al., 2002). One intracellular kinase then allosterically activates the other, resulting in phosphorylation of C-terminal tyrosines (Zhang et al., 2006) (Figure 1A). Phosphorylated tyrosines recruit signaling adapters such as Shc, Grb2, and SOS, which stimulate a variety of downstream pathways (Margolis et al., 1989). Among these, the Ras-MAPK (mitogen-activated protein kinase) pathway is a particularly important regulator of cell behaviors such as proliferation and migration.

The formation of phosphorylated EGFR dimers is generally considered sufficient to initiate Ras signaling because the dimers recruit the Ras-GEF (guanine nucleotide exchange factor) SOS to the membrane, and membrane-localized SOS is sufficient to activate Ras under a variety of conditions (Aronheim et al., 1994; Christensen et al., 2016; Toettcher et al., 2013). However, conflicting observations raise questions regarding whether a phosphorylated dimer is a competent signaling unit, sufficient to activate Ras, in the absence of EGF. For example, dimerization of a chimeric receptor's intracellular domains with rapamycin derivatives was sufficient to induce EGFR phosphorylation and downstream Erk phosphorylation (Muthuswamy et al., 1999). In contrast, dimerization of EGFR on cancer cell lines with therapeutic antibodies resulted in phosphorylated EGFR but no Erk phosphorylation (Yoshida et al., 2008). While these examples varied greatly in experimental design—for instance, the antibodies specifically targeted EGFR's extracellular domain and locked EGFR dimers in an inactive conformation (Li et al., 2005), whereas the chimeric EGFR had its extracellular domain replaced with the

This is an open access article under the CC BY-NC-ND license (http://creativecommons.org/licenses/by-nc-nd/4.0/).

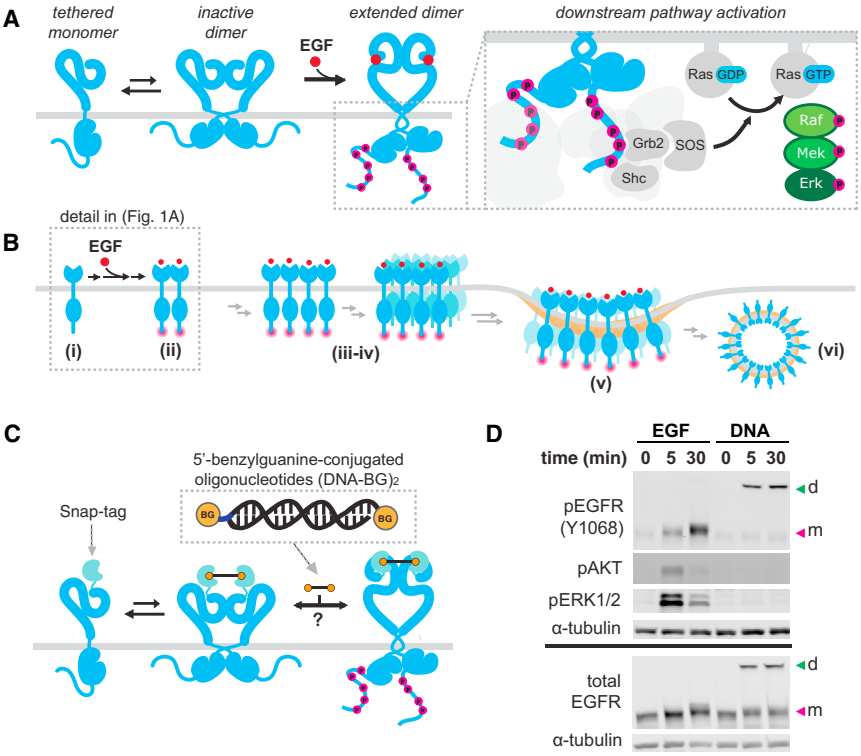

Figure 1. Decoupling EGFR Dimerization and Transphosphorylation from Other EGF-Induced Conformational and Spatial Changes

(A) EGFR exists in a tethered monomer or an inactive dimer formation. Upon EGF binding, it adopts an extended dimer conformation and undergoes auto-transphosphorylation. Phosphorylated dimers recruit adaptor proteins to EGFR, resulting in activation of the Ras-MAPK pathway.

(B) EGF binding to EGFR also results in rapid changes in spatial organization from monomers (i) to dimers (ii); to higher order multimers and nanoscale clusters (iii-iv); to micron scale clusters in clathrin-coated pits (v); and, finally, to endosomes (vi).

(C) A chemical genetic system utilizing a SNAP-tag on the N terminus of full-length EGFR and BG-modified DNA dimers as crosslinkers.

(D) Representative western blot of lysates from cells treated with 8 nM EGF or 2 μM $(DNA\text{-}BG)_2$. To maintain DNA hybridization, SDS-PAGE samples were not boiled. EGFR dimers (d) and monomers (m) are indicated with arrows.

transmembrane and extracellular domain of p75 Neurotrophin receptor—it remains difficult to rationalize how the phosphorylated intracellular domains could be signaling competent in one study but not in another.

A possible resolution of this conundrum is the requirement for a specific tertiary or quaternary structure beyond the dimer, promoted by EGF binding, to efficiently activate Ras. Upon EGF binding, dimers undergo rapid spatial rearrangement into oligomers and nanoscale clusters (Figure 1B) (Ariotti et al., 2010; Clayton et al., 2008; Ichinose et al., 2004; Saffarian et al., 2007; van Lengerich et al., 2017), and these oligomers may promote downstream signaling (Huang et al., 2016; Kozer et al., 2013; Needham et al., 2016). However, because oligomerization and signaling changes occur on a similar timescale, it remains unclear whether specific spatial intermediates are a cause or consequence of downstream signaling.

We sought to determine whether a phosphorylated EGFR dimer is sufficient to activate Ras signaling without EGF. This question is challenging to answer, because receptor overexpression (Avraham and Yarden, 2011; Pedersen et al., 2005), mutations and truncations (Arkhipov et al., 2013; Bessman et al., 2014), and antibodies (Li et al., 2005; Schmiedel et al., 2008) can perturb the conformations adopted by EGFR and have unpredictable consequences on signaling. We addressed these challenges by developing a chemical genetic strategy based on targeted chemical crosslinking that allows for the preparation of a clean population of full-length receptor dimers, expressed at near-WT (wild-type) levels, and dimerized using long and flexible crosslinkers that do not significantly restrict receptor conformations. This strategy effectively decouples EGFR dimerization from other EGF-induced conformation changes and dynamics, allowing us to conclude that the critical function of EGF in Ras signal transduction is not limited to promoting the formation of a phosphorylated EGFR dimer, but also promoting receptor dynamics, conformations, or oligomeric states necessary for downstream signaling.

RESULTS

A Chemical Genetic System for Preparing Full-Length EGFR Dimers without Ligand

To decouple EGF-induced receptor dimerization from other EGF-induced conformation changes, we sought to exploit the equilibrium between monomers and inactive dimers on resting cells. We hypothesized that selectively reducing the off rate of EGFR dimers would stimulate autophosphorylation rates sufficient to overcome high endogenous levels of background phosphatase activity (Kleiman et al., 2011), thereby generating phosphorylated receptor dimers. First, we modified the N terminus of full-length EGFR with a flexible linker and a SNAP-tag, which rapidly forms a covalent bond with benzyl guanine (BG), as the chemical dimerization domain. When this construct was stably expressed in HEK293 cells at physiological levels, we found that it was efficiently activated by the addition of nanomolar concentrations of EGF (Figure 1D). For the chemical dimerizer, we incorporated BG at the 5′-hydroxyl of double-stranded DNA molecules $(DNA\text{-}BG)_2$, (20-mer; approximate length, 6.8 nm; Figure 1C). Addition of $(DNA\text{-}BG)_2$ to live cells for 5 or 30 min resulted in a higher molecular weight band by western blot, consistent with a trapped dimeric species (Figures 1D and S1). Blotting for phosphorylation of tyrosine 1068 confirmed that the kinase domains of trapped dimers were active. Strikingly, we also observed pronounced differences in phosphorylated Erk between EGF-stimulated and trapped dimer receptors

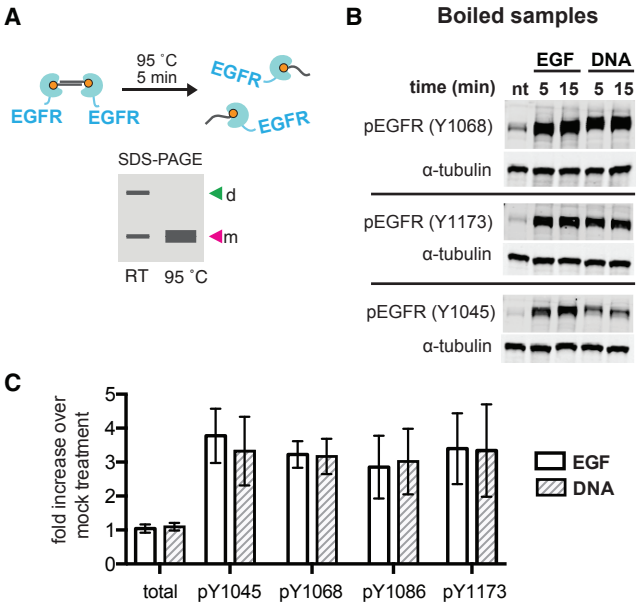

Figure 2. Quantitative Comparison of Tyrosine Phosphorylation after Dimerization by EGF or (DNA-BG)$_2$

(A) DNA-dimerized receptors can be revealed by PAGE without boiling or can be boiled to reveal a monomer for direct comparison to EGFR monomers. d, dimer; m, monomer; RT, room temperature.

(B) Representative western blot of boiled lysates from cells treated with serum-free media (nt, no treatment), 8 nM EGF or 2 μM (DNA-BG)$_2$ at various tyrosines.

(C) Mean fold increase of total EGFR and phosphotyrosines upon EGF or (DNA-BG)$_2$ treatment compared to no treatment control (n = 3; error bars indicate SD).

(Figure 1D). Consistently, and in multiple cell lines, we observed strong Erk and Akt signaling from EGF-stimulated SNAP-EGFR, and no signaling above background in the presence of (DNA-BG)$_2$ (Figure S1). These results suggest that selective stabilization of an EGFR dimer is sufficient to stimulate kinase activity independent of additional conformational changes associated with EGF binding. However, receptor phosphorylation alone did not generate Ras-MAPK signaling.

Trapped EGFR Dimers Are Phosphorylated to a Similar Extent as EGF-Activated EGFR

Differences in EGFR phosphorylation levels between (DNA-BG)$_2$ and EGF stimuli, as well as the pattern of phosphorylation (Ronan et al., 2016), could explain differences in downstream Erk activation. This hypothesis could be tested by quantitative western blotting, but quantitative comparison can be challenging between monomeric and crosslinked species, because large differences in molecular weight impact the transfer efficiency of proteins (Towbin et al., 1979). We therefore selectively melted (DNA-BG)$_2$ crosslinks by boiling samples after cell lysis but prior to SDS-PAGE (Figure 2A).

Using the concentration of EGF and (DNA-BG)$_2$ in Figure 1D, which gave EGFR phosphorylation in both conditions but Erk phosphorylation only with EGF, we used quantitative western blotting to compare the phosphorylation levels of a suite of tyrosines: Y1045, Y1068, Y1086, and Y1173. Notably, we observed phosphorylation to a similar extent for both conditions (Figures 2B and 2C) at a time point and EGF concentration sufficient for propagation of downstream signals. Increasing the concentration of (DNA-BG)$_2$ gives a similar result, illustrating the crosslinker was working near saturating conditions (Figure S2).

Phosphorylated EGFR Dimers Are Not Sufficient to Stimulate Ras Activation

Mechanistically, several steps occur between the formation of a phosphorylated EGFR dimer and Erk activation. We therefore sought to identify the specific step at which the signaling capacity of EGF- and (DNA-BG)$_2$-stimulated dimers diverged. Because Erk activation requires Ras-GTP formation, we first investigated whether signaling breakdown occurred at or before the level of Ras activation. To evaluate the activation status of Ras, we used the Ras-binding domain of Raf, which selectively binds Ras-GTP, to pull down GTP-bound activated Ras from whole-cell lysates. We used the same concentrations of EGF and (DNA-BG)$_2$ as in our earlier assays and confirmed that, while EGF and (DNA-BG)$_2$ stimulated similar levels of Y1068 phosphorylation after 5 min, only EGF-activated EGFR was capable of activating Erk signaling. Analyzing the same lysates for Ras activation, we observed efficient pulldown of Ras-GTP in EGF-treated cells, while little to no Ras-GTP was detected in cells treated with (DNA-BG)$_2$ (Figures 3A and 3B). This was particularly surprising, given that Y1068 is widely considered the primary site responsible for recruiting the Grb2/Sos complex that activates Ras (Yamauchi et al., 1997). Thus, phosphorylated EGFR dimers are not sufficient to activate Ras.

Trapped EGFR Dimers Recruit Key Adaptor Proteins for Ras Signaling

An inability to activate Ras could be explained by an inability of phosphorylated EGFR to recruit core signaling adaptors such as SOS, Shc, and Grb2. We therefore investigated adaptor recruitment to EGF-stimulated and trapped dimer receptors using co-immunoprecipitation. We treated SNAP-EGFR-expressing cells with EGF or (DNA-BG)$_2$ to generate similar levels of phosphorylated receptor, immunoprecipitated the total EGFR, and then compared the quantity of adaptor proteins that co-precipitated after 5 min. Surprisingly, we did not observe a difference in the quantity of precipitated Grb2, SOS, and Shc between receptors stimulated with EGF or (DNA-BG)$_2$, despite striking changes in the level of Ras-GTP observed under the same conditions (Figures 3C–3F). These results show that differential recruitment of core adaptor proteins to EGFR cannot explain the differences in Ras signaling between our two conditions.

The Structure and Charge of the Crosslinker Do Not Significantly Impact EGFR Transphosphorylation or Signal Propagation

Given these surprising findings, we next investigated whether (DNA-BG)$_2$ was contributing to the lack of Ras signaling in trapped EGFR dimers. Adding the reagents sequentially, with (DNA-BG)$_2$ followed by EGF, resulted in Erk and Akt activation (Figure S2), suggesting that (DNA-BG)$_2$ was not broadly inactivating EGFR. Next, we removed both charge and rigidity from the dimerizer by substituting the nucleic acid portion of (DNA-BG)$_2$ with a highly flexible and uncharged polyethylene glycol

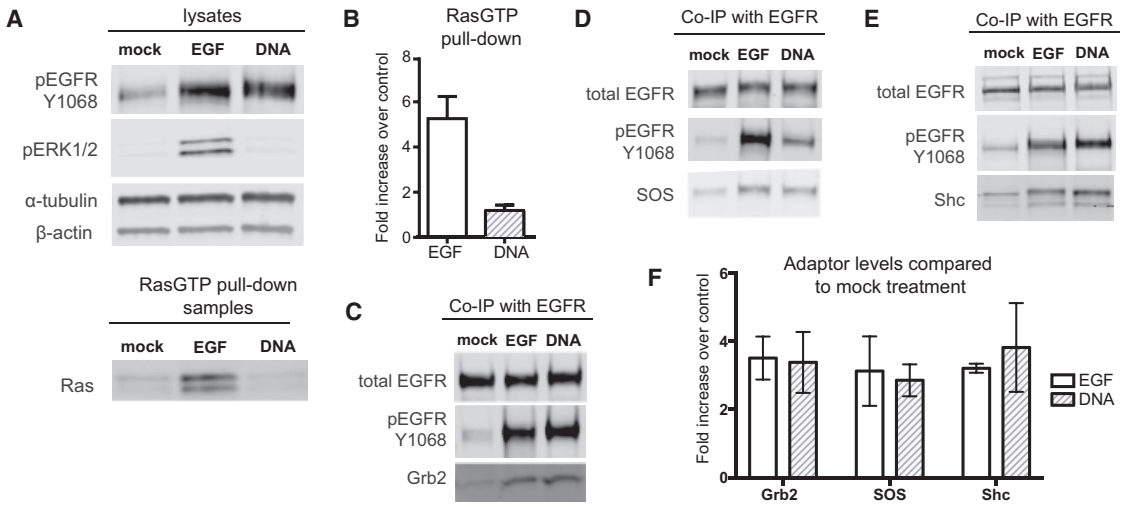

Figure 3. Trapped EGFR Dimers Recruit Adaptors with Similar Stoichiometry to EGF-Stimulated Cells but Do Not Activate Ras

(A) Representative western blot showing lysates from cells treated with either 8 nM EGF, 2 μM $(DNA\text{-}BG)_2$, or serum-free media (mock) for 5 min. The same lysates were used in a RasGTP pull-down, and samples were blotted for total Ras.

(B) Mean RasGTP levels in each treatment compared to negative control (n = 3; error bars indicate SD).

(C) Representative blot of Grb2 co-immunoprecipitation (coIP) with EGFR on lysates from treated cells.

(D) Representative blot of SOS coIP with EGFR.

(E) Representative blot of Shc coIP with EGFR.

(F) Quantification of adaptor coIP in treated cells compared to negative controls. Signals for each adaptor were normalized to total EGFR levels in the pull-down sample and plotted as mean fold increase over mock treatment (n = 3; error bars indicate SD).

(PEG) molecule. Treatment of SNAP-EGFR-expressing cells with $PEG_{26}\text{-}BG_2$ triggered efficient formation of phosphorylated dimers but no Erk phosphorylation to levels above control (Figure S2). Similar results were observed for shorter PEG crosslinkers, including PEG_9 and PEG_5. Moreover, crosslinking a mutant EGFR (V924R), which is unable to form active asymmetric kinase dimers, did not result in receptor phosphorylation (Figure S2). These findings demonstrate that crosslinkers activate the receptor by promoting canonical interactions between the kinase domains but that they are deficient in their ability to promote specific EGF-dependent active conformations necessary for Ras activation.

We also considered that the irreversible nature of BG-based crosslinker dimerization versus reversible EGF-induced dimerization could be a factor in the difference in downstream signaling. To address this, we made versions of the 20-bp $(DNA\text{-}BG)_2$ with only 6, 8, or 10 contiguous complementary bases to increase the off rate of the duplex. If the irreversibility of crosslinks was the explanation of the observed defect in signaling, we would expect an increase in Erk phosphorylation per unit of receptor phosphorylation as the duplex melting temperature approached 37°C. However, we did not observe an increase with any of the mismatched duplexes (Figure S2).

Phosphorylation of EGFR Dimers Is Not Sufficient for Nanoscale Oligomer Formation

Our findings demonstrate that, when EGFR dimers are trapped with linkers that do not significantly constrain receptor conformation, they can autophosphorylate and recruit key signaling adapters such as SOS but, surprisingly, do not stimulate Ras. We therefore sought to better understand how trapped receptor dimers might differ from EGF-induced complexes in events downstream of receptor phosphorylation, such as oligomerization and trafficking. We investigated this question by imaging cells treated with $(DNA\text{-}BG)_2$ or EGF using stochastic optical reconstruction microscopy (STORM). We used an EGFR construct with a photoswitchable fluorescent protein (mEos 3.2) fused to the C terminus to resolve oligomers that might only be visible by imaging below the diffraction limit and expressed this construct at levels similar to those of receptors in previous experiments (Figure S1). We observed that, upon the addition of $(DNA\text{-}BG)_2$ to SNAP-EGFR-mEos-expressing cells, the spatial arrangement of receptors was similar to that of unstimulated controls, whereas receptors stimulated with EGF led to rapid accumulation of bright foci after 10 min (Figures 4A and S3). We quantified images of cells treated with media alone, EGF, or $(DNA\text{-}BG)_2$ and constructed pairwise distance histograms for each condition. A peak in the histogram indicates an increase in receptor local density compared to random at a given length scale. Compared to untreated cells, we found an increase in the histogram height (indicative of increased dimers and small oligomers) as well as width (indicative of the formation of larger oligomers) in cells treated with EGF. In contrast, the analysis of receptor distribution in the $(DNA\text{-}BG)_2$-treated cells showed only a modest increase in histogram height, consistent with an increased dimer fraction, but no increase in histogram width, indicative of no change in the size of clusters when compared to untreated cells (Figure 4B).

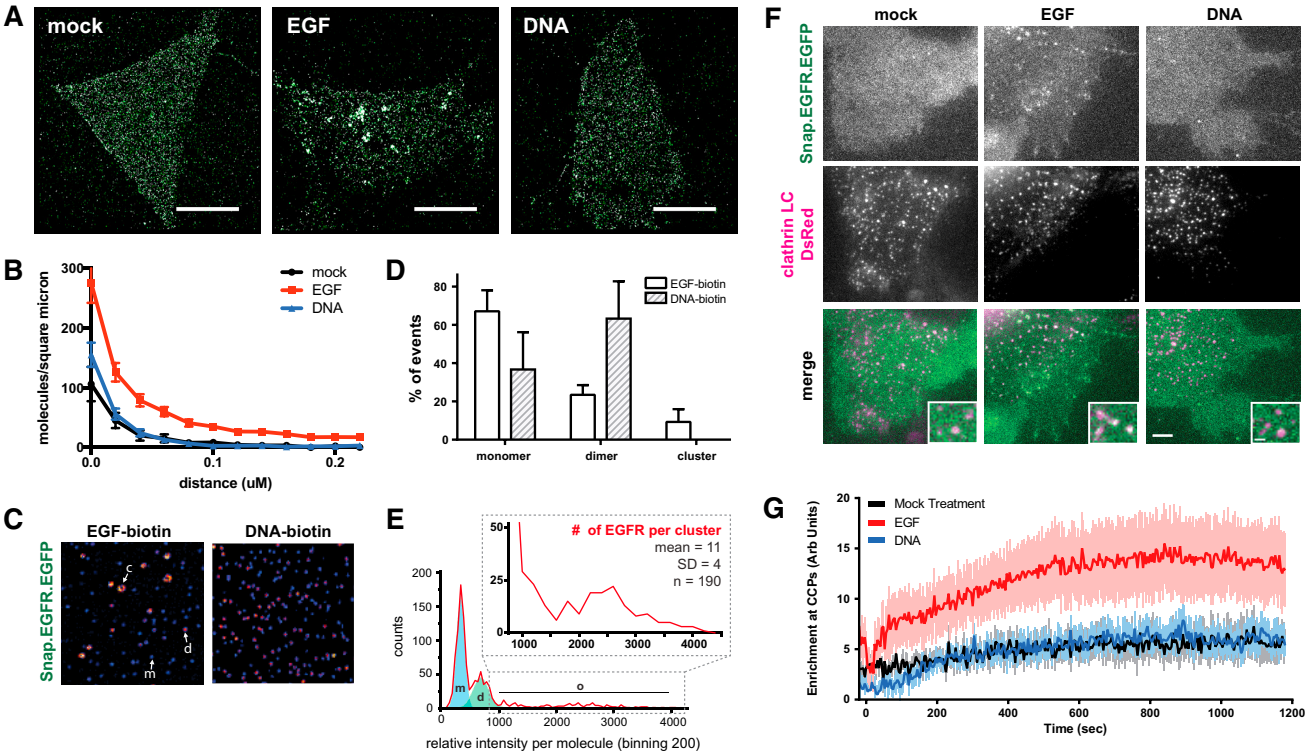

Figure 4. Trapped EGFR Dimers Do Not Form Nanoscale Spatial Intermediates or Traffic to Clathrin-Coated Pits

(A) Representative images of HEK293-SNAP-EGFR-mEos cells incubated with serum-free media (mock), 8 nM EGF or 2 μM $(DNA-BG)_2$ for 10 min and then imaged by STORM. Scale bars, 10 μm.

(B) Pairwise correlation analysis of STORM images graphed as median and standard error (n = 10 cells per condition).

(C) Representative images of single-molecule IP of SNAP-EGFR-EGFP cells treated with biotin (bt)-EGF or bt-$(DNA-BG)_2$ for 5 min. Ligand-bound receptors from lysates were immobilized on neutravidin-coated slides and imaged. EGFR monomers (m) appear as blue spots, dimers (d) appear as pink spots, and clusters (c) appear as larger yellow spots.

(D) Mean monomer, dimer, and cluster populations of EGFR graphed as a percentage of the sample (n = 3 independent experiments; error bars indicate SD).

(E) Representative EGF-biotin-treated sample with counts of relative intensity per molecule. The blue shaded region represents the monomer portion, the green shaded region represents the dimer portion, and zoom represents the cluster portion. The average number of EGFR molecules per cluster was estimated by dividing the average intensity of the clusters by the intensity of a monomer.

(F) TIRF images of HEK293 cells co-transfected with SNAP-EGFR-EGFP and clathrin-light chain-dsRed after treatment with 8 nM EGF, 2 μM DNA, or serum-free media at 15 min. Scale bar, 1 μm.

(G) Enrichment of SNAP-EGFR-EGFP at clathrin-coated pits over time after treatment with 8 nM EGF, 2 μM $(DNA-BG)_2$, or serum-free media graphed as mean and SD (n = 10 cells per condition).

To further investigate the degree of oligomerization, we performed single-molecule precipitation of SNAP-EGFR-EGFP receptors treated with biotinylated EGF or biotinylated $(DNA-BG)_2$ after 5 min. We precipitated Triton X-100-disrupted cells onto neutravidin-coated slides as previously described (Lee et al., 2013) to immobilize ligand-bound receptor complexes, and we imaged the intensity of individual fluorescent spots as a proxy for the number of EGFR molecules in each complex (Figure 4C). We observed an increased ratio of dimers to monomers in both conditions compared to controls but uniquely observed the formation of multiple brighter spots only when cells were treated with biotinylated-EGF (Figure 4D). Comparing the fluorescence intensity of these spots to those of the putative monomer and dimer peaks suggested an average cluster size of approximately 7–15 molecules for EGF-stimulated receptors (Figure 4E) after 5 min.

In addition to studying receptor arrangements at fixed time points, we also imaged the dynamic reorganization of EGFR on live cells. To do so, we used total internal reflection fluorescence (TIRF) microscopy to follow the EGFR trafficking in real time, using clathrin-coated pits as a frame of reference. Although non-clathrin mediated endocytosis may contribute to EGFR dynamics under certain conditions, we found that a significant fraction of EGF-stimulated receptors were recruited to clathrin-coated pits at the EGF concentration used in our studies, whereas the localization of $(DNA-BG)_2$-treated receptors was largely unchanged compared to controls over the course of 20 min (Figures 4F, 4G, and S4). Therefore, EGF triggers conformational changes in the EGFR that are necessary for the oligomerization of phosphorylated receptors and their reorganization on live-cell membranes.

DISCUSSION

If EGFR oligomerization and other cell-surface dynamics are necessary for efficient MAPK signal transduction, how might they be coupled to Ras activity? EGFR oligomerization could stimulate Ras activity by concentrating Ras and SOS in common signaling complexes, thereby increasing their effective molarity relative to broadly distributed GAPs, and cooperatively stimulating the formation of Ras-GTP. Consistent with this model, Ras dimerization and nanoclustering have been shown to affect downstream Erk signaling (Nan et al., 2015; Tian et al., 2007; Zhou et al., 2014). Alternatively, EGF binding may cause changes in EGFR transmembrane conformation associated with clustering and the formation of lipid microdomains required for signaling. For example, EGFR clusters have been shown to colocalize with membrane regions enriched for PIP_2(4,5) (Laketa et al., 2014), and the GEF activity of SOS can be modulated by charged lipids, including PIP_2(4,5) (Gureasko et al., 2008; Zhao et al., 2007).

Independent of the detailed mechanism, our findings have important implications for understanding the regulation of Ras—and, possibly, other signaling molecules—by EGFR. We can conclude that conformational changes and/or other processes associated with EGF binding are necessary for oligomer formation and that these higher order EGFR oligomers may be more potent activators of Ras, on a molecule-to-molecule basis, when compared to phosphorylated dimers. Such EGF-dependent formation of EGFR nanoclusters may add an additional layer of spatial regulation to growth factor signaling, which aligns with an emerging view of how Ras regulates downstream pathways, through the formation of similar higher order species. Our findings also emphasize that not all EGFR dimers (or oligomers) are the same, and, depending on the initiating signal, receptor activation may evolve very differently. For example, a recent elegant dissection of structural and functional properties of EGFR dimers induced by different ligands suggests that more stable receptor dimers induce more transient profiles of receptor phosphorylation and downstream pathway activation, presumably by being long lived enough to recruit negative-feedback regulators (Freed et al., 2017). Our findings argue that, in addition to the kinetics of receptor activation, the spatial distribution of receptors following their activation is a critical determinant of downstream signal propagation. Long-lived trapped dimers are signaling deficient not because they fail to accumulate substantial phosphorylation and recruit adapters but, perhaps, because tertiary or quaternary interaction are structurally incompatible with subsequent organization into effective signaling platforms. Finally, our results demonstrate that receptor activation and signal transduction can be mechanistically decoupled. This finding has important implications for the development of future therapeutics, which could specifically target receptor organization rather than activation to modulate signal transduction through specific pathways.

EXPERIMENTAL PROCEDURES

Details are provided in the Supplemental Information.

Cell Signaling Assays

Cells stably expressing SNAP-EGFR were grown to 70%–80% confluency and then serum starved for 6–8 hr prior to stimulus with EGF or $(DNA\text{-}BG)_2$ at 37°C, lysed, and prepared for western blots. For quantitative western blotting, secondary antibodies conjugated to either Alexa Fluor 680 or DyLight 800 were used, and blots were imaged on a LI-COR Biosciences imaging system. Scans were quantified and analyzed by densitometry. Measurements were normalized to loading controls and shown as the mean and SD of 3 independent experiments.

STORM

HEK293-SNAP-EGFR-mEos cells were serum starved for 6 hr and then incubated with the indicated stimuli at 37°C for 10 min. Cells were fixed and imaged with an inverted microscope using TIRF illumination, 100× magnification, and a 561-nm laser at 60 Hz. Once every 10 frames, mEos was converted from green to red state with 405-nm illumination. Images from 10 cells per condition were corrected for blinking as previously described (Puchner et al., 2013), and the molecular positions were then used to calculate all the pairwise distances as previously described (van Lengerich et al., 2017).

Single-Molecule IP

HEK293-SNAP-EGFR-EGFP cells were treated with 8 nm of EGF-biotin or 2 μM of $(BG\text{-}DNA)_2$-biotin for 5 min at 37°C, and then lysed with 1% Triton X-100 buffer. Lysates were incubated on neutravidin-coated PEG slides and imaged by TIRF microscopy. Over 3 independent experiments, monomer, dimer, and cluster populations were identified by bleaching steps and analysis of pixel intensity histograms.

Clathrin Colocalization

HEK293 cells were transfected with SNAP-EGFR-EGFP and clathrin light chain-dsRed using Lipofectamine 2000. Cells were imaged 48 hr later, live at 37°C with various stimuli. SNAP-EGFR-EGFP enrichment at clathrin structures was calculated as the difference between the average fluorescence inside and outside regions enriched for dsRed. Each condition represents 10 cells pooled across 7 independent experiments.

SUPPLEMENTAL INFORMATION

Supplemental Information includes Supplemental Experimental Procedures and four figures and can be found with this article online at https://doi.org/10.1016/j.celrep.2018.02.031.

ACKNOWLEDGMENTS

We thank the Gartner lab members for insightful discussions. We thank B. Huang, K. Shokat, J. Taunton, P. England, and D. Fujimori for sharing instruments and facilities. This work is supported by an Achievement Rewards for College Scientists fellowship and a Genentech Foundation fellowship to S.I.L., an American Cancer Society postdoctoral fellowship (124801-PF-13-365-01-TBE) to B.v.L., a grant from the National Institute of General Medical Sciences (R01 GM109176) to N.J., a UCSF CTSI-SOS pilot grant (1 UL1 RR024131-01), an NIGMS Systems Biology Center grant (P50 GM081879), NSF grant MCB-1330864, and the NSF Center for Cellular Construction (DBI-1548297). Z.J.G. is a Chan Zuckerberg Biohub Investigator. M.C. and T.-Y.Y. were supported by the Institute for Basic Science (IBS; IBS-R0216-D1).

AUTHOR CONTRIBUTIONS

S.I.L. and Z.J.G. conceived the study. S.I.L., Z.J.G., and N.J. supervised the study and drafted the manuscript. B.v.L. and S.I.L. cloned plasmids and made cell lines. S.I.L. and D.M.P. made the chemical dimerizers. S.I.L. performed cell-signaling assays. B.v.L. performed STORM. K.E. performed live TIRF. M.C. performed single-molecule IP. T.-Y.Y. and M.v.Z. provided key insight and additional supervision for experiments. All authors contributed to writing and editing the final manuscript.

DECLARATION OF INTERESTS

The authors declare no competing interests.

Received: September 17, 2017
Revised: December 25, 2017
Accepted: February 7, 2018
Published: March 6, 2018

REFERENCES

Ariotti, N., Liang, H., Xu, Y., Zhang, Y., Yonekubo, Y., Inder, K., Du, G., Parton, R.G., Hancock, J.F., and Plowman, S.J. (2010). Epidermal growth factor receptor activation remodels the plasma membrane lipid environment to induce nanocluster formation. Mol. Cell. Biol. *30*, 3795–3804.

Arkhipov, A., Shan, Y., Das, R., Endres, N.F., Eastwood, M.P., Wemmer, D.E., Kuriyan, J., and Shaw, D.E. (2013). Architecture and membrane interactions of the EGF receptor. Cell *152*, 557–569.

Aronheim, A., Engelberg, D., Li, N., al-Alawi, N., Schlessinger, J., and Karin, M. (1994). Membrane targeting of the nucleotide exchange factor Sos is sufficient for activating the Ras signaling pathway. Cell *78*, 949–961.

Avraham, R., and Yarden, Y. (2011). Feedback regulation of EGFR signalling: decision making by early and delayed loops. Nat. Rev. Mol. Cell Biol. *12*, 104–117.

Bessman, N.J., Freed, D.M., and Lemmon, M.A. (2014). Putting together structures of epidermal growth factor receptors. Curr. Opin. Struct. Biol. *29*, 95–101.

Christensen, S.M., Tu, H.-L., Jun, J.E., Alvarez, S., Triplet, M.G., Iwig, J.S., Yadav, K.K., Bar-Sagi, D., Roose, J.P., and Groves, J.T. (2016). One-way membrane trafficking of SOS in receptor-triggered Ras activation. Nat. Struct. Mol. Biol. *23*, 838–846.

Chung, I., Akita, R., Vandlen, R., Toomre, D., Schlessinger, J., and Mellman, I. (2010). Spatial control of EGF receptor activation by reversible dimerization on living cells. Nature *464*, 783–787.

Clayton, A.H.A., Orchard, S.G., Nice, E.C., Posner, R.G., and Burgess, A.W. (2008). Predominance of activated EGFR higher-order oligomers on the cell surface. Growth Factors *26*, 316–324.

Ferguson, K.M., Berger, M.B., Mendrola, J.M., Cho, H.S., Leahy, D.J., and Lemmon, M.A. (2003). EGF activates its receptor by removing interactions that autoinhibit ectodomain dimerization. Mol. Cell *11*, 507–517.

Freed, D.M., Bessman, N.J., Kiyatkin, A., Salazar-Cavazos, E., Byrne, P.O., Moore, J.O., Valley, C.C., Ferguson, K.M., Leahy, D.J., Lidke, D.S., and Lemmon, M.A. (2017). EGFR ligands differentially stabilize receptor dimers to specify signaling kinetics. Cell *171*, 683–695.e18.

Gureasko, J., Galush, W.J., Boykevisch, S., Sondermann, H., Bar-Sagi, D., Groves, J.T., and Kuriyan, J. (2008). Membrane-dependent signal integration by the Ras activator Son of sevenless. Nat. Struct. Mol. Biol. *15*, 452–461.

Huang, Y., Bharill, S., Karandur, D., Peterson, S.M., Marita, M., Shi, X., Kaliszewski, M.J., Smith, A.W., Isacoff, E.Y., and Kuriyan, J. (2016). Molecular basis for multimerization in the activation of the epidermal growth factor receptor. eLife *5*, e14107.

Ichinose, J., Murata, M., Yanagida, T., and Sako, Y. (2004). EGF signalling amplification induced by dynamic clustering of EGFR. Biochem. Biophys. Res. Commun. *324*, 1143–1149.

Jura, N., Endres, N.F., Engel, K., Deindl, S., Das, R., Lamers, M.H., Wemmer, D.E., Zhang, X., and Kuriyan, J. (2009). Mechanism for activation of the EGF receptor catalytic domain by the juxtamembrane segment. Cell *137*, 1293–1307.

Kleiman, L.B., Maiwald, T., Conzelmann, H., Lauffenburger, D.A., and Sorger, P.K. (2011). Rapid phospho-turnover by receptor tyrosine kinases impacts downstream signaling and drug binding. Mol. Cell *43*, 723–737.

Kozer, N., Barua, D., Orchard, S., Nice, E.C., Burgess, A.W., Hlavacek, W.S., and Clayton, A.H.A. (2013). Exploring higher-order EGFR oligomerisation and phosphorylation–a combined experimental and theoretical approach. Mol. Biosyst. *9*, 1849–1863.

Laketa, V., Zarbakhsh, S., Traynor-Kaplan, A., Macnamara, A., Subramanian, D., Putyrski, M., Mueller, R., Nadler, A., Mentel, M., Saez-Rodriguez, J., et al. (2014). PIP_3 induces the recycling of receptor tyrosine kinases. Sci. Signal. *7*, ra5.

Lee, H.-W., Kyung, T., Yoo, J., Kim, T., Chung, C., Ryu, J.Y., Lee, H., Park, K., Lee, S., Jones, W.D., et al. (2013). Real-time single-molecule co-immunoprecipitation analyses reveal cancer-specific Ras signalling dynamics. Nat. Commun. *4*, 1505.

Li, S., Schmitz, K.R., Jeffrey, P.D., Wiltzius, J.J.W., Kussie, P., and Ferguson, K.M. (2005). Structural basis for inhibition of the epidermal growth factor receptor by cetuximab. Cancer Cell *7*, 301–311.

Margolis, B.L., Lax, I., Kris, R., Dombalagian, M., Honegger, A.M., Howk, R., Givol, D., Ullrich, A., and Schlessinger, J. (1989). All autophosphorylation sites of epidermal growth factor (EGF) receptor and HER2/neu are located in their carboxyl-terminal tails. Identification of a novel site in EGF receptor. J. Biol. Chem. *264*, 10667–10671.

Muthuswamy, S.K., Gilman, M., and Brugge, J.S. (1999). Controlled dimerization of ErbB receptors provides evidence for differential signaling by homo- and heterodimers. Mol. Cell. Biol. *19*, 6845–6857.

Nan, X., Tamgüney, T.M., Collisson, E.A., Lin, L.-J., Pitt, C., Galeas, J., Lewis, S., Gray, J.W., McCormick, F., and Chu, S. (2015). Ras-GTP dimers activate the mitogen-activated protein kinase (MAPK) pathway. Proc. Natl. Acad. Sci. USA *112*, 7996–8001.

Needham, S.R., Roberts, S.K., Arkhipov, A., Mysore, V.P., Tynan, C.J., Zanetti-Domingues, L.C., Kim, E.T., Losasso, V., Korovesis, D., Hirsch, M., et al. (2016). EGFR oligomerization organizes kinase-active dimers into competent signalling platforms. Nat. Commun. *7*, 13307.

Ogiso, H., Ishitani, R., Nureki, O., Fukai, S., Yamanaka, M., Kim, J.-H., Saito, K., Sakamoto, A., Inoue, M., Shirouzu, M., and Yokoyama, S. (2002). Crystal structure of the complex of human epidermal growth factor and receptor extracellular domains. Cell *110*, 775–787.

Pedersen, M.W., Pedersen, N., Damstrup, L., Villingshøj, M., Sønder, S.U., Rieneck, K., Bovin, L.F., Spang-Thomsen, M., and Poulsen, H.S. (2005). Analysis of the epidermal growth factor receptor specific transcriptome: effect of receptor expression level and an activating mutation. J. Cell. Biochem. *96*, 412–427.

Puchner, E.M., Walter, J.M., Kasper, R., Huang, B., and Lim, W.A. (2013). Counting molecules in single organelles with superresolution microscopy allows tracking of the endosome maturation trajectory. Proc. Natl. Acad. Sci. USA *110*, 16015–16020.

Ronan, T., Macdonald-Obermann, J.L., Huelsmann, L., Bessman, N.J., Naegle, K.M., and Pike, L.J. (2016). Different epidermal growth factor receptor (EGFR) agonists produce unique signatures for the recruitment of downstream signaling proteins. J. Biol. Chem. *291*, 5528–5540.

Saffarian, S., Li, Y., Elson, E.L., and Pike, L.J. (2007). Oligomerization of the EGF receptor investigated by live cell fluorescence intensity distribution analysis. Biophys. J. *93*, 1021–1031.

Schmiedel, J., Blaukat, A., Li, S., Knöchel, T., and Ferguson, K.M. (2008). Matuzumab binding to EGFR prevents the conformational rearrangement required for dimerization. Cancer Cell *13*, 365–373.

Tian, T., Harding, A., Inder, K., Plowman, S., Parton, R.G., and Hancock, J.F. (2007). Plasma membrane nanoswitches generate high-fidelity Ras signal transduction. Nat. Cell Biol. *9*, 905–914.

Toettcher, J.E., Weiner, O.D., and Lim, W.A. (2013). Using optogenetics to interrogate the dynamic control of signal transmission by the Ras/Erk module. Cell *155*, 1422–1434.

Towbin, H., Staehelin, T., and Gordon, J. (1979). Electrophoretic transfer of proteins from polyacrylamide gels to nitrocellulose sheets: procedure and some applications. Proc. Natl. Acad. Sci. USA *76*, 4350–4354.

van Lengerich, B., Agnew, C., Puchner, E.M., Huang, B., and Jura, N. (2017). EGF and NRG induce phosphorylation of HER3/ERBB3 by EGFR using

distinct oligomeric mechanisms. Proc. Natl. Acad. Sci. USA *114*, E2836–E2845.

Yamauchi, T., Ueki, K., Tobe, K., Tamemoto, H., Sekine, N., Wada, M., Honjo, M., Takahashi, M., Takahashi, T., Hirai, H., et al. (1997). Tyrosine phosphorylation of the EGF receptor by the kinase Jak2 is induced by growth hormone. Nature *390*, 91–96.

Yoshida, T., Okamoto, I., Okabe, T., Iwasa, T., Satoh, T., Nishio, K., Fukuoka, M., and Nakagawa, K. (2008). Matuzumab and cetuximab activate the epidermal growth factor receptor but fail to trigger downstream signaling by Akt or Erk. Int. J. Cancer *122*, 1530–1538.

Zhang, X., Gureasko, J., Shen, K., Cole, P.A., and Kuriyan, J. (2006). An allosteric mechanism for activation of the kinase domain of epidermal growth factor receptor. Cell *125*, 1137–1149.

Zhao, C., Du, G., Skowronek, K., Frohman, M.A., and Bar-Sagi, D. (2007). Phospholipase D2-generated phosphatidic acid couples EGFR stimulation to Ras activation by Sos. Nat Cell Biol. *9*, 706–712.

Zhou, Y., Liang, H., Rodkey, T., Ariotti, N., Parton, R.G., and Hancock, J.F. (2014). Signal integration by lipid-mediated spatial cross talk between Ras nanoclusters. Mol. Cell. Biol. *34*, 862–876.

Cell Reports, Volume *22*

Supplemental Information

Phosphorylated EGFR Dimers

Are Not Sufficient to Activate Ras

Samantha I. Liang, Bettina van Lengerich, Kelsie Eichel, Minkwon Cha, David M. Patterson, Tae-Young Yoon, Mark von Zastrow, Natalia Jura, and Zev J. Gartner

SUPPLEMENTAL FIGURES AND LEGENDS

Fig. S1: SNAP-EGFR expressed at low levels has low background phosphorylation and is responsive to EGF in multiple cell lines, related to Figure 1 (A) Uncropped western blot from figure 1D shown at one scan intensity with labeled MW ladder. (B) Representative FACS plots of wild-type HEK293 cells and cells after stable transduction with SNAP-EGFR and selection by FACS sorting. The HEK293 cells used in signaling assays were sorted for low expression to achieve low background phosphorylation of EGFR in the absence of treatment. Cells were lifted with PBS without Ca^{2+} and Mg^{2+}, with 0.04% EDTA, and labeled with 1 µM BG-Alexafluor488 for 30 minutes on ice. (C) Quantum MESF beads were used to quantify surface receptor number counts on SNAP-EGFR cell lines that were labeled with a non-cell permeable BG-Alexafluor dye and analyzed by flow cytometry. Error bars are standard deviation of three separate experiments. (D) Western blot of H1299 cells stably expressing SNAP-EGFR and treated with either 8 nM of EGF or 2 µM $(DNA\text{-}BG)_2$. (E) Western blot of murine suspension Ba/F3 cells stably expressing SNAP-EGFR and treated with either 8 nM of EGF or 2 µM $(DNA\text{-}BG)_2$. (F) Western blot of breast epithelial MCF10A cells stably expressing SNAP-EGFR and treated with either 8 nM of EGF or 2 µM $(DNA\text{-}BG)_2$.

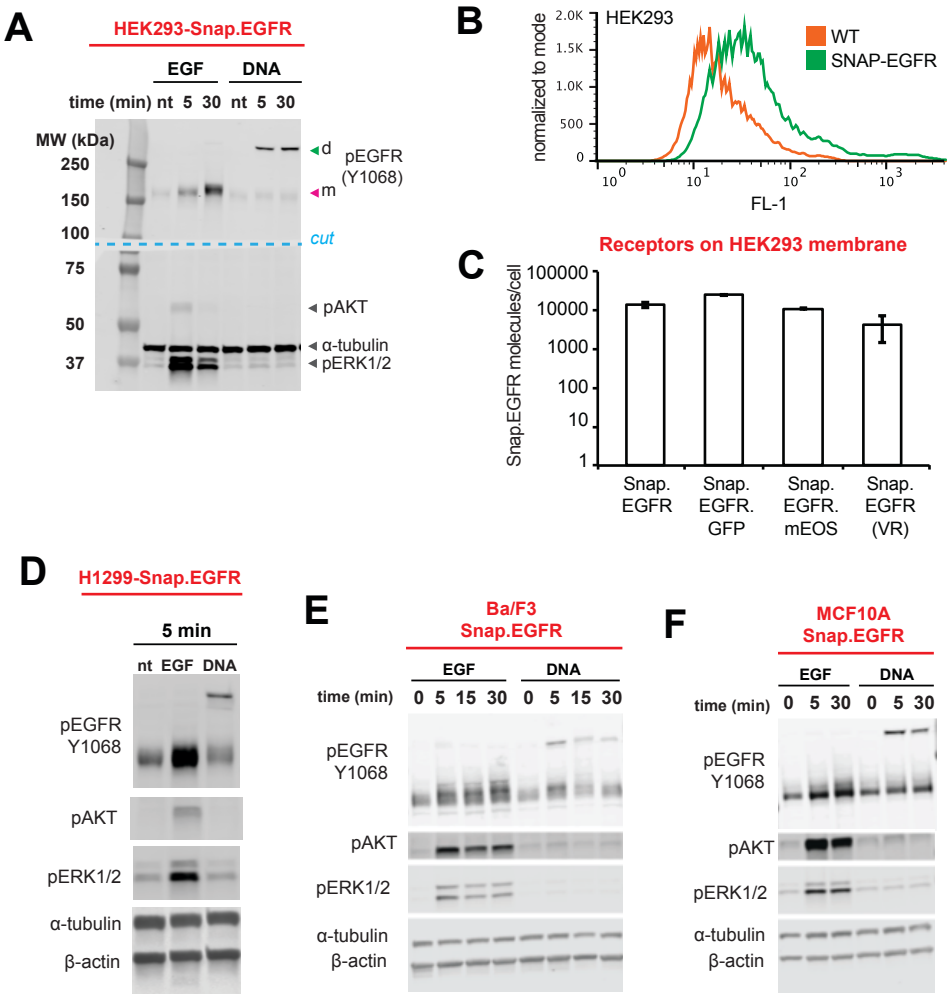

Fig. S2: EGFR phosphorylation occurs without ERK or AKT activation when the structure of chemical cross-linkers is altered, related to Figure 1. (A) Western blot of cells treated with different lots of $(DNA\text{-}BG)_2$ at 2 µM as well as double the $(DNA\text{-}BG)_2$ concentration at 4 µM. No pERK was observed at either concentration of $(DNA\text{-}BG)_2$ compared to stimulation with 8 nM EGF. (B) Western blot of cells stimulated with either 8 nM of EGF, 2 µM $(DNA\text{-}BG)_2$, or sequential addition $(DNA\text{-}BG)_2$ and EGF. For sequential addtion, 2 µM $(DNA\text{-}BG)_2$ was first added to cells for 15 minutes, then 8 nM EGF was added for the indicated times. (C) Quantitation of pERK levels from the conditions described in (B) in relation to EGF-treated cells. pERK levels were normalized to loading controls and baseline levels of pERK, and then plotted as the percent of the value of pERK for cells treated with EGF for 5 minutes. Error bars are standard deviation of three independent experiments. (D) Western blot of cells treated with flexible and uncharged BG-dimerizers, which were synthesized from PEGs of the indicated lengths. Approximate PEG lengths are 2 nm (n = 5), 3.6 nm (n = 9), 10.5 nm (n=26). EGFR phosphorylation was observed without ERK or AKT activation with these PEG-based crosslinkers. (E) Cells expressing SNAP.EGFR and cells expressing mutant SNAP.EGFR(V942R) were both treated with EGF and BG-PEG_{26}-BG for 5 minutes. (F) Western blot of cells treated with 20mer DNA duplexes having 6, 8, 10, and 20 contiguous complementary bases designed to decrease the lifetime of the duplex. T_m of the pairs are included in the SI with the corresponding DNA sequences. No increase in pERK signal was observed for any of the duplexes.

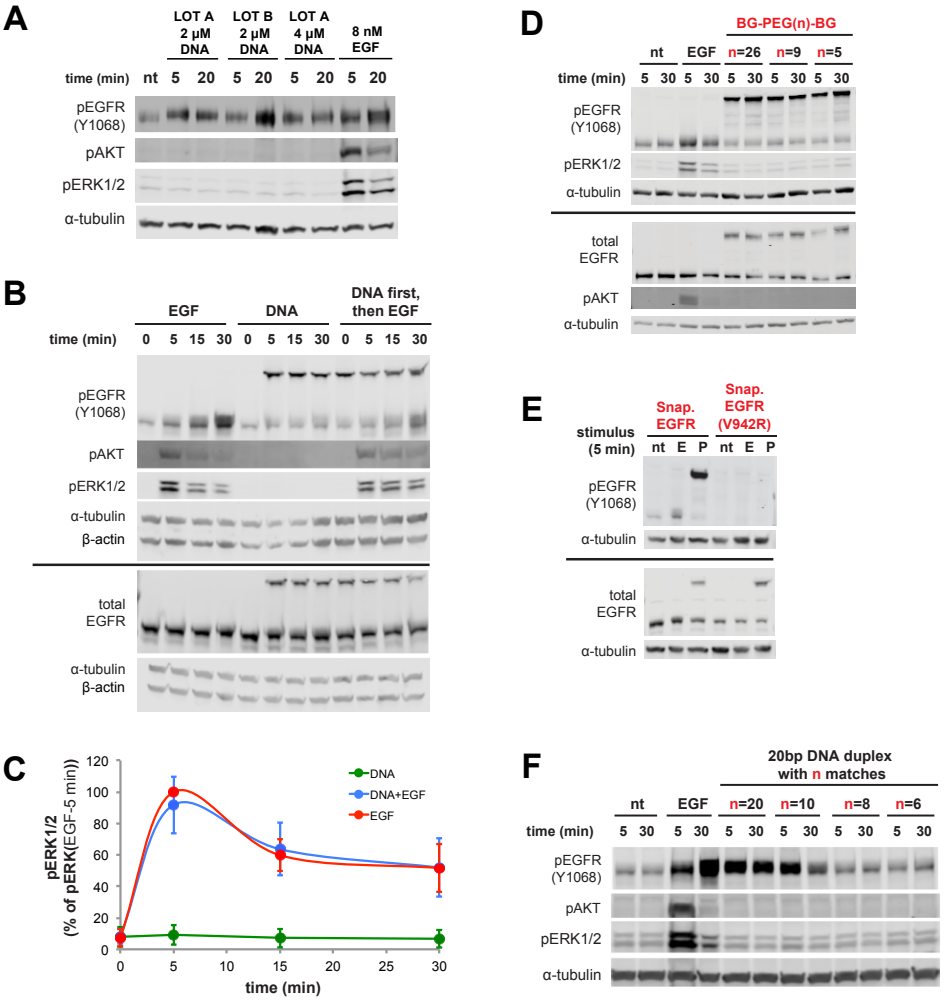

Fig. S3: Panel of representative images of HEK293-SNAP-EGFR-mEos cells (related to Figure 4) were incubated with 8 nM EGF, 2 μM $(DNA\text{-}BG)_2$, or serum-free media (no treatment) for 10 minutes. Cells were imaged by STORM and images in Figure 6a are included here in larger form, along with another set of representative images. Scale bar is 10 μm.

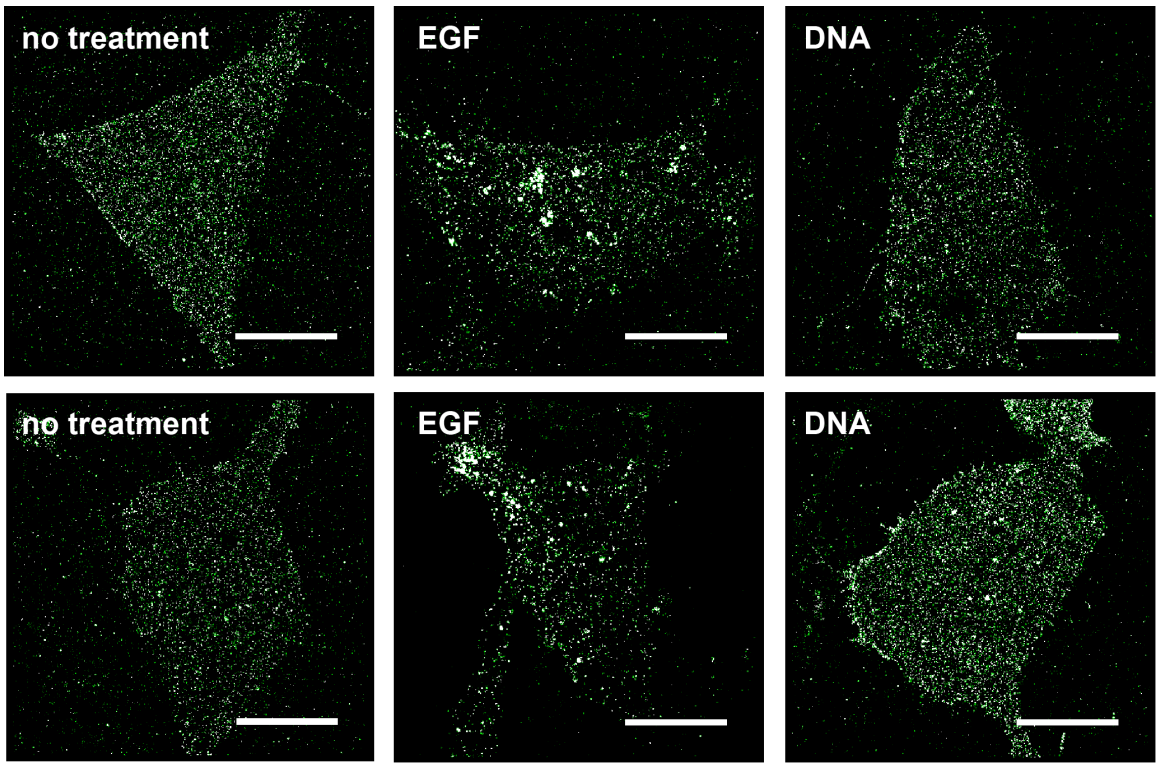

Fig. S4: Representative images of Snap-EGFR-EGFP co-localization to clathrin coated pits, related to Figure 4. (A) TIRF images of HEK293 cells co-transfected with SNAP-EGFR-EGFP and clathrin-light chain-dsRed after treatment with 8 nM of EGF at time points from 0-20 minutes. (B) 2 μM of DNA, (C) or media as a mock treatment. Scale bars are 1 micron.

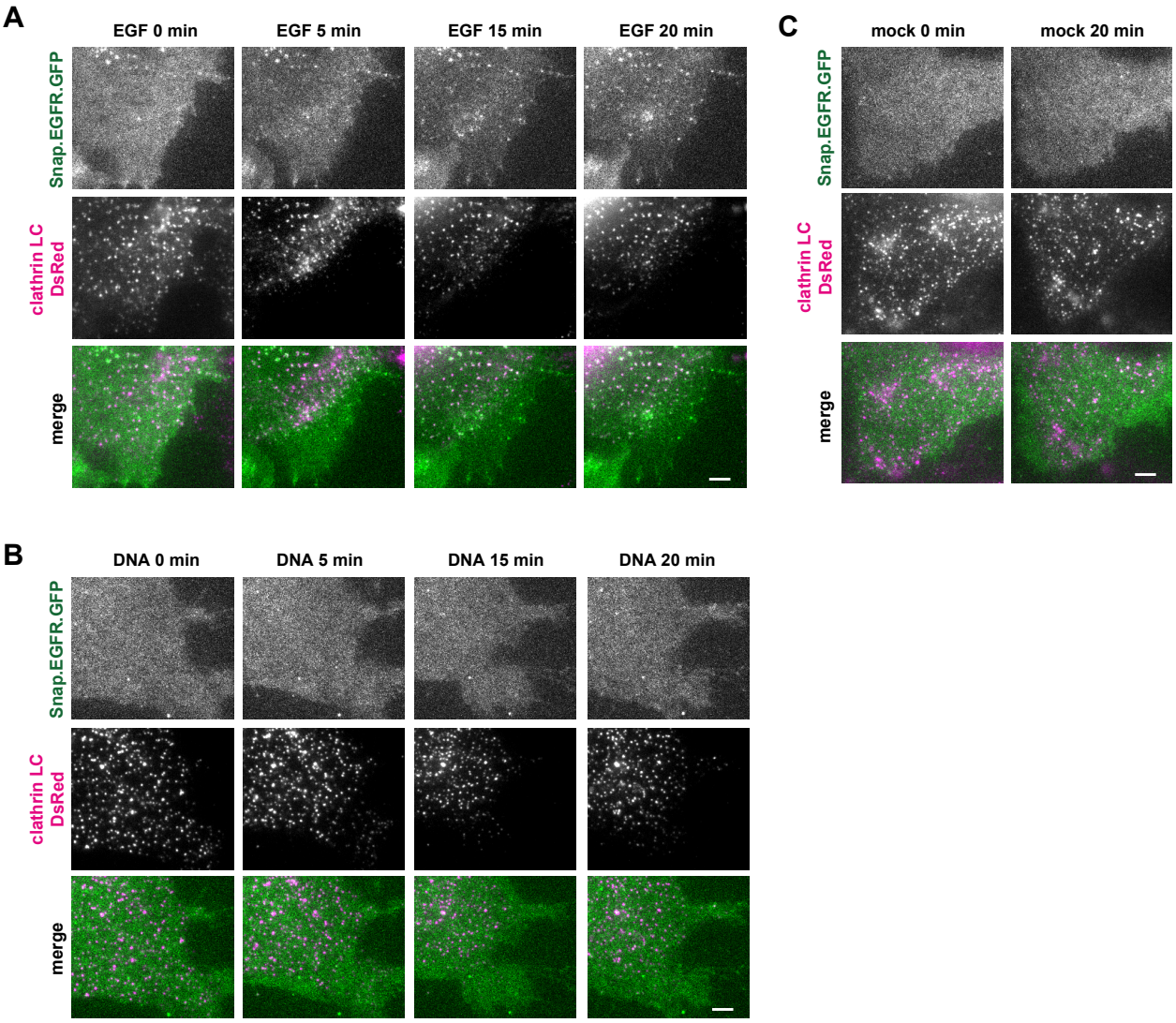

SUPPLEMENTAL EXPERIMENTAL PROCEDURES

Synthesis of benzylguanine-modified oligonucleotides

Benzylguanine-conjugated N-Hydroxysuccinimide (BG-GLA-NHS) was purchased from New England Biolabs. All phosphoramidites and DNA synthesis reagents and solvents were purchased from Glen Research. Amine-modified oligonucleotides were synthesized on an Applied Biosystems Expedite 8909 DNA synthesizer using a default coupling protocol, with the addition of a 5'-Amino-Modifier C6 phosphoramidite (Glen Research, cat. # 10-1906) resuspended at 100 mM as the last step. CPG beads from up to five 1 µmol syntheses of amine-modified DNA were aliquoted among several microcentrifuge tubes. 2 mg of the BG-GLA-NHS ester was dissolved in 400 µl of dry DMSO (Sigma Aldrich), mixed with 100 µl of dry N,N-Diisopropylethylamine (DIPEA, Sigma Aldrich) under argon, and then quickly transferred evenly among the microcentrifuge tubes to completely submerge the CPG beads. The microcentrifuge lids were secured with parafilm and the reaction agitated on a vortex mixer overnight. The beads were then washed 3 times with dimethylformamide (DMF, Sigma Aldrich), 3 times with dichloromethane (DCM, Sigma Aldrich), 1 time with acetonitrile, and then dried completely on a speed vac system. In order to maintain the BG, a mild cleavage solution without methylamine was used. The DNA was cleaved off the beads using a mixture of 30% ammonium hydroxide for 2 hours at 65 °C, dried on a speed vac system, resuspended in 100 mM triethylamine acetate (TEAA), and filtered through 0.2-µm spin filters. The BG-conjugated strand with a 3' conjugated biotin was prepared similarly, but using biotin-TEG-conjugated CPG support from Glen Research (cat. # 20-29550).

Oligonucleotides were then purified by reversed-phase high-performance liquid chromatography (Agilent 1260 Infinity Series HPLC System) using a 5 um Eclipse XDB-C18 9.4 x 250 mm column (Agilent). An elution gradient of 8-15% acetonitrile in 100 mM TEAA (pH7) over 20 minutes, followed by a gradient of 15-70% acetonitrile over 6 minutes, was used to purify BG-DNA, which eluted around 22-23 minutes from the start of the program. Fractions containing BG-modified oligonucleotides were washed with Millipore MilliQ-purified water and lyophilized three times. Prior to use, the DNA was resuspended in water and its concentration was determined by its absorbance at 260 nM measured on a NanoDrop (Thermo Scientific).

DNA sequences were selected as previously described (Hsiao et al., 2009) to form dimer constructs with minimal secondary structure and are listed below:

Name	Sequence	calculated Tm*
BG-20A	Benzylguanine-5'-GTAACGATCCAGCTGTCACT-3'	66.28 ˚C
BG-20A'	Benzylguanine -5'-AGTGACAGCTGGATCGTTAC-3'	
BG-20A-biotin	Benzylguanine -5'-AGTGACAGCTGGATCGTTAC-3'-biotin	
BG-20A'-MM10	Benzylguanine -5'-gtaagCAGCTGGATCtcact-3'	51.26 ˚C
BG-20A'-MM12	Benzylguanine -5'-gtaacgAGCTGGATgtcact-3'	37.64 ˚C
BG-20A'-MM14	Benzylguanine -5'-gtaagttGCTGGAcgtcact-3'	26.28 ˚C

*calculated at 2 µM concentration, 154 mM Na^+, 0.81 mM Mg^{2+} and considering only the directly complementary sequence shown in caps.

Synthesis of benzylguanine-modified PEG linkers

All reagents and solvents were purchased from commercial sources and used as received without further purification. Reactions were carried out under an inert atmosphere of argon in flame-dried glassware. Reactions were purified by HPLC using an Agilent 1200 series liquid chromatography system with Agilent Eclipse XDB C-18 5 µm, 4.6 x 250 mm column. An elution gradient of 5-90% acetonitrile in 0.1% aqueous trifluoroacetic acid over 25 minutes was used for purification. Mass spectrometry was performed on a LC-MS (Waters Acquity UPLC/ESI-TQD) with the Acquity BEH C18 1.7 um, 2.1x50 mm column.

Synthesis of bis(BG)-PEG26 crosslinker: O,O'-Bis(2-aminoethyl)hexacosaethylene glycol (1.5 mg, 1.2 µmol, Santa Cruz Biotechnology) was dissolved in anhydrous dimethylsulfoxide (0.5 mL). A drop of N,N-diisopropylethylamine was added to the solution followed by addition of BG-GLA-NHS (2.0 mg, 4.15 µmol). The solution was allowed to stir at room temperature overnight. The reaction mixture was concentrated under reduced pressure, redissolved in 3:1 water:acetonitrile, filtered and purified via HPLC. The purified sample was lyophilized to yield the desired product (0.65 mg, 0.33 µmol, 28% yield): MS (LC-MS) *m/z* calculated for $C_{92}H_{152}N_{14}O_{33}$ [M+H]+ 1982.07, found 1982.54.

Synthesis of bis(BG)-PEGn crosslinker: $BS(PEG)_n$ (9 μmol, Thermo Fisher Scientific) was dissolved in anhydrous dimethylsulfoxide (37.5 μL). N,N-diisopropylethylamine (70 μL, 0.4 mmol) was added to the solution followed by addition of 6-((4-(aminomethyl)benzyl)oxy)-7H-purin-2-amine (54 mg, 0.2 mmol). The solution was allowed to stir at room tempearture overnight. The reaction mixture was concentrated under reduced pressure, redissolved in 3:1 water:acetonitrile, filtered and purified via HPLC. The purified sample was lyophilized to yield the desired product.

Bis(BG)-PEG_5. (1.7 mg, 2.0 μmol, 22% yield) MS (LC-MS) *m/z* calculated for $C_{40}H_{50}N_{12}O_9$ [M+H]+ 843.39, found 843.83.
Bis(BG)-PEG_9. (2.1 mg, 2.1 μmol, 23% yield) MS (LC-MS) *m/z* calculated for $C_{48}H_{68}N_{12}O_{13}$ [M+H]+ 1020.50, found 1020.03.

Plasmids and generation of stable cell lines
Lentiviral plasmids for SNAP-EGFR, SNAP-EGFR-EGFP, and SNAP-EGFR(VR) were cloned into the DT39 vector by Gibson assembly using a homemade mixture. In each case, the signal peptide was fused in front of the SNAP protein to guide membrane localization. The backbone DT39 was a generous gift from the Weiner lab at UCSF, and the Snap construct was a generous gift of the Huang lab. The open reading frames of the signal peptide, the SNAP protein, and the remainder of EGFR, and GFP, were amplified by PCR and purified by agarose gel. Each piece contained 25 bp homology to its neighboring piece or the vector, and the pieces were assembled by Gibson assembly. The VR mutant was made by quick change of the wild type construct. The plasmid for SNAP-EGFR-mEos was made by replacing the DNA sequence encoding GFP from the SNAP-EGFR-EGFP plasmid with a DNA sequence encoding mEOS amplified using an enzymatic inverse PCR strategy. Lentivirus or retrovirus plasmids were prepared in larger scale using the Qiagen Midi-prep kit and delivered to UC San Francisco's Viracore for lentivirus production. Cells were transduced by plating at 25% confluency on 10 cm diameter tissue culture plates and incubating in 5 ml of media with 250 ul of virus at 37 ˚C. After 6-24 hours, 5 ml of media with 10% serum were added to the cells. The virus-containing media was replaced with fresh media after 48 hr, and the cultures split after 72 hours. HEK293 and H1299 cells were cultured with DMEM-H21 (UCSF Cell Culture Facility) with 10% FBS (UCSF Cell Culture Facility). MCF10A cells were cultured with DMEM/F12 (UCSF Cell Culture Facility), 5% horse serum (UCSF Cell Culture Facility), 20 ng/ml EGF (Peprotech), 0.5 μg/ml hydrocortisone (Sigma-Aldrich), 100 ng/ml cholera toxin (Sigma-Aldrich), and 10 μg/ml insulin (Invitrogen). Ba/F3 cells were cultured in RPMI (UCSF Cell Culture Facility) with 10% FBS and 1 ng/ml mouse IL-3 (Invitrogen).

In order to generate cell lines with low levels of SNAP-EGFR, SNAP-EGFR(VR), SNAP-EGFR-EGFP, and SNAP-EGFR-mEOS expression, transduced cells were subjected to a round of fluorescence activated cell sorting (FACS). Cells were lifted with Ca^{2+} and Mg^{2+} free PBS containing 0.04% EDTA, then incubated in PBS with 1 μM of BG-Alexafluor488 dye (New England Biolabs) for 10 minutes at 37 ˚C. Then the cells were washed 3 times with PBS with 1% BSA and resuspended in 1 ml of PBS with 1% BSA. Cells were then analyzed on the Facs Aria III (BD Biosciences) and sorted into 4 populations based on their level of fluorescence above non-transduced control cells. All cell signaling assays and STORM assays were performed using the 25% of cells incorporating the lowest amount of dye, as these cells were to have the lowest levels of background EGFR signaling. The number of SNAP-EGFR and SNAP-EGFR(VR) receptors were quantified on HEK293 cells using Quantum MESF 488 microspheres (Bangs Laboratories, Inc.) after cell labeling with 1 μM BG-Alexafluor 488 (New England Biolabs) for 30 minutes on ice. SNAP-EGFR-EGFP and SNAP-EGFR-mEOS receptors were quantified on HEK293 cells using Quantum MESF 647 microspheres (Bangs Laboratories, Inc.) after cell labeling with 1 μM BG-Alexafluor 647 (New England Biolabs) for 30 minutes on ice. Cells were then washed with PBS with 1% BSA three times and analyzed on a Facs Calibur (BD Biosciences), using the Quantum MESF microspheres to generate a standard curve for the total number of AF488 or AF647 molecules based on fluorescence intensity.

Cell signaling assays
6X stocks of the stimuli (EGF, $(BG\text{-}DNA)_2$, BG-PEG-BG) were prepared prior to all experiments in serum free media: 6X BG-DNA stock (12 uM); 6X BG-PEG-BG stock (12 uM); 6X EGF stock (300 ng/ml, 48 nM). 1X lysis buffer (20 mM Tris-HCl (pH 7.5), 150 mM Na_2EDTA, 1 mM EGTA, 1% Triton, 2.5 mM sodium pyrophosphate, 1 mM β-glycerophosphate, 1 mM Na_3VO_4, and 1 μg/ml leupeptin) was prepared by diluting a 10X stock (Cell Signaling Technologies) and adding 1 tablet of phosphatase inhibitor cocktail (PhosSTOP, Roche) and 1 tablet of protease inhibitor cocktail (cOmplete Mini, Roche). Cells were typically cultured in 12-well plates until 70-80% confluency. They were then serum starved with 1 ml of serum-free DMEM-H21 for 6-8 hours so as to achieve the lowest possible level of background phosphorylation of EGFR/ERK/AKT. Before stimulating the cells, they were

washed and placed in 250 µl of serum-free media. 50 ul of pre-warmed 6X stocks were then added to each well to initiate the experiment. Cells were moved onto ice, quickly washed 2 times with ice cold PBS, and lysed in 60 ul of lysis buffer on ice for 15 minutes. The cells were scraped off the plates with the back of a pipette tip, and the lysates were transferred to microcentrifuge tubes and centrifuged at 13000xg 10 minutes at 4 ^{o}C in order to pellet out insoluble cell debris. The supernatant were then transferred to a new tube and 4X Laemmli sample buffer (Bio-Rad, 277.8 mM Tris-HCL (pH6.8), 44.4% (v/v) glycerol, 4.4% lithium dodecyl sulfate, 0.02% bromophenol blue) with 250 µM DTT or 10% BME as a reducing agent was added to the lysates. Lysates were stored at -20 ^{o}C and efforts were taken to minimize freeze thaw cycles. A similar protocol was used for co-immunoprecipitation experiments, but using a 10 cm culture plate.

Western blotting and analysis

For western blots, samples were loaded onto BioRad 4-15% gradient TGX gels in SDS-PAGE buffer (25 mM Tris, 192 mM glycine, 0.1% SDS). For denatured $(BG\text{-}DNA)_2$-treated samples where BG-DNA-modified EGFR runs as a monomer, the lysates were boiled immediately before loading on the gel. The gels are run at 250V for 35 minutes resulting in warm buffer throughout electrophoresis. For non-DNA denatured samples, the lysates run at 200V for 45-60 minutes in pre-chilled running buffer that maintained a cool temperature throughout electrophoresis. All western blots are transferred using a BioRad Criterion wet transfer system onto nitrocellulose membranes (BioRad) in a Tris-Glycine buffer (25 mM Tris-HCL, 192 mM glycine) with 20% methanol. Blots were transferred at 150V in ice cold buffer for 25 or 27 minutes for a monomer or dimer transfer, respectively. The blots are then washed briefly with 1X TBST (150 mM NaCl, 20 mM Tris Base, pH 7.4, 0.1% Tween 20) and the blocked in 5% non-fat milk solids in TBST for at least 1 hour at room temperature with gentle rocking. The blots are then washed 3 times with 1X TBST and incubated in the primary antibody overnight on a rocker.

The following rabbit primary antibodies were used at 1:1000 in 5% BSA in TBST: EGFR (D38B1 XP, Cell Signaling Technologies), pEGFR Y1068 (clone D7A5 XP, Cell Signaling Technologies), pEGFR Y1045 (#2237, Cell Signaling Technologies), pEGFR Y1086 (#2220, Cell Signaling Technologies), pEGFR Y1173 (clone 53A5, Cell Signaling Technologies), pERK1/2 Thr202/Tyr204 (clone D13.14.4E XP, Cell Signaling Technologies), pAKT Ser473 (clone D9E XP, Cell Signaling Technologies), and clathrin heavy chain (clone TD.1, Santa Cruz Biotechnology). The loading control mouse antibodies alpha-tubulin (clone DM1A, Sigma-Aldrich) and beta-actin (clone AC-15, Sigma-Aldrich, or similar) were used at 1:10000 in 5% BSA. Following incubation with primary antibody, the blots were then washed 4 times for 5 minutes each in 1X TBST. Then, they were incubated in secondary antibodies conjugated to either AlexaFluor680 (Thermo Fisher Scientific) or DyLight800 (Thermo Fisher Scientific and Rockland) diluted 1:10000 into 5% milk in TBST for 1-2 hours at room temperature, protected from light. After 3 more washes in 1X TBST, the blots were imaged on a Licor imaging system. Scans were then quantified and analyzed on ImageStudioLite (Licor) by densitometry. Measurements were normalized to the geometric mean of the intensity of both loading controls alpha-tubulin and beta-actin.

Ras-activation assay

Ras-GTP was precipitated from lysates using an Active Ras Pull-Down and Detection Kit (Thermo Fisher Scientific). Cells were plated at 80% confluency in a 10 cm dish and serum starved for 6.5 hours. The media was removed and replaced with 5 ml of the indicated ligand as a 1X solution in serum free media, and incubated for five minutes at 37 ^{o}C. The plates were then placed on ice, washed twice with ice cold PBS, and lysed using 500 µl of the 1X lysis buffer included in the kit with protease and phosphatase inhibitor cocktail tablets added. The cells incubated on ice for 15 minutes, then scraped off the plates with the back of a pipette tip, and the lystates were transferred to microcentrifuge tubes and centrifuged at 13000xg 10 minutes at 4 ^{o}C in order to pellet out insoluble cell debris. 30 µl of the fresh lysate was reserved and added to 12 µl of 4X SDS-PAGE buffer containing BME to run as a lysate reference. Ras-GTP was precipitated from crude lysates using an Active Ras Pull-Down and Detection Kit (Thermo Fisher Scientific). Briefly, 100 µl of a 50% slurry of Glutathione Resin was put into a spin cup with a collection tube, washed with 400 µl of lysis buffer, and centrifuged. 400 µl of lysate was then added to the spin cups, which were then capped on both ends and incubated at 4 ˚C while rotating for 1 hour. The spin cup was then unsealed, centrifuged again and the resin was washed 3 more times with lysis buffer. For elution, 50 µl of 2X SDS sample buffer with BME was added to the resin, vortexed, and incubated at room temperature for 2 minutes. The spin tube was then transferred to a fresh collection tube and the flow through was collected. The eluted samples were then heated for 5 minutes at 95 ˚C. For the western blot analysis, 25 µl of each sample was loaded on a gel and the anti-Ras antibody provided in the kit was used to detect Ras.

Co-immunoprecipitation with EGFR

Lysates were prepared as described above for the Ras-GTP Pull Down assay. 250 µl of lysis buffer was added to 150 µl of lysate, 5.5 µl of a mouse anti-EGFR antibody (#2256, Cell Signaling Technology), and incubated at 4 ˚C overnight while on a rotary mixer. The next day, 40 µl of a Protein G-conjugated magnetic bead slurry (#8740, Cell Signaling Technology) was added to the tubes and incubated at 4 ˚C for 2 hours while on a rotary mixer. The beads were then washed 4 times with 500 µl of 1X lysis buffer using a magnetic rack. Proteins were eluted by incubating the beads with 60 µl of 2X sample buffer, quickly vortexed, and boiled for 5 minutes. Finally, the tubes were centrifuged at 13000 g for 1 minute and the supernatant was transferred to a new tube. For the western blot analysis, 20 µl of the samples were run in each lane of the gel and the protocol described above was used with the following primary antibodies at a 1:250 dilution in 5% BSA in TBST: Grb2 (#3972, Cell Signaling Technologies), SHC (ab24787, Abcam), and SOS (clone D3T7T, Cell Signaling Technologies). The same samples were also probed with total EGFR and phosphorylated-EGFR antibodies as controls to ensure that similar amounts of total EGFR were pulled down in each sample.

Live cell total internal reflection fluorescence microscopy (TIR-FM) imaging and analysis

TIR-FM was performed at 37 °C using a Nikon Ti-E inverted microscope equipped for through-the-objective TIR-FM and outfitted with a temperature-, humidity-, and CO_2-controlled chamber (Okolab). Images were obtained with an Apo TIRF 100X, 1.49 numerical aperture objective (Nikon) with solid-state lasers of 488 and 561 nm (Keysight Technologies). An Andor iXon DU897 EMCCD camera controlled by NIS-Elements 4.1 software was used to acquire image sequences every 4 seconds for 20 minutes. Cells were transfected with SNAP-EGFR-EGFP and clathrin light chain-dsRed (CLC-dsRed) using Lipofectamine 2000 (Life Technologies) according to manufacture protocol 48 hours before imaging and then plated on poly-L-lysine (0.0001%, Sigma) coated 35-mm glass-bottomed culture dishes (MatTek Corporation) 24 hours before imaging. Prior to imaging, cells were washed once and imaged live in DMEM without phenol red (UCSF Cell Culture Facility) supplemented with 30 mM HEPES, pH 7.4. Cells were treated as indicated at frame 5 of 301 image sequences. Acquired image sequences were saved as stacks of 16 bit TIFF files. Receptor fluorescence enrichment into clathrin-coated structures (CCSs) was calculated using a mask of CCSs generated using a thresholded average image of the clathrin channel as previously described (Eichel et al., 2016). Enrichment at CCSs was measured as the difference between the average fluorescence in the mask and average fluorescence outside of the thresholded structures. Each condition represents 10 cells pooled across 7 independent experiments.

Stochastic Optical Reconstruction Microscopy (STORM) and analysis

8-well chambered coverglass slides (Lab-tek) were cleaned with 1 M KOH for 10 minutes, then washed and coated with poly-lysine (0.01%) for 30 minutes. Stably infected HEK293 cell lines expressing SNAP-EGFR- mEos3.2 were deposited on the washed glass slide, and allowed to adhere for 36 hours. Cells were serum starved for six hours, then incubated for with serum-free media (control), 8 nM EGF, or 2 uM DNA at 37°C for 10 minutes. Cells were fixed with 4% formaldehyde for 10 minutes at 20 °C, washed, and stored in PBS at 4 °C. Fixed cells were imaged using an inverted microscope at 100x magnification and TIRF illumination. Cells were located in the 488 nm (green) channel and then imaged with STORM in the 561 nm (red) channel at 60 Hz, and mEos photoconversion from the green to red state was achieved with 405 nm illumination (once every ten frames). Images were processed using custom scripts, and were corrected for blinking as previously described (Puchner et al., 2013). Blinking-corrected molecular positions were then used to calculate a corrected pair-correlation histogram, which calculates all the pair-wise distances as previously described (van Lengerich et al., 2017). This histogram is further corrected for average density by subtracting the average baseline value (calculated as the average from 500 nm to 1000 nm) from the function. This allowed the peak height and width among different conditions to be compared directly, since different samples may contain slightly different density of molecules. To display cluster size histograms, the blink-corrected molecular positions were subjected to an algorithm that counted the number of neighboring molecules within a certain cut-off radius (here, 50 nm was used, which is the FWHM of the measurement).

Single Molecule Immunoprecipitation and Imaging

HEK293 cells stably transduced with SNAP-EGFR-EGFP were plated at 80% confluency and serum starved for 6.5 hours. Cells were then treated with either 8 nm of EGF-biotin or 2 uM of $(BG\text{-}DNA)_2$ for 5 minutes at 37 ˚C and then lysed. Lysates of HEK293 cells with SNAP-EGFR-EGFP were prepared by dissolving the cells with Triton X-100 lysate buffer (1% Triton X-100, 50 mM Tris-Hcl, 150 mM Nacl, 1 mM EDTA, 10% Glycerol). The supernatant of the lysis buffer was then collected after centrifugation at 15000xg. We then precipitated Triton-X100 disrupted cells onto neutravidin coated slides as previously described (Jain et al., 2011; Lee et al., 2013). In more detail, we immobilized the SNAP-EGFR-EGFP receptors bound with bt-EGF or bt-DNA), we prepared Neutravidin-coated

(0.5 mg/ml) PEG slides. SNAP-EGFR-EGFP in the lysate was pulled down on Neutravidin-coated PEG slides and imaged with by TIRF microscopy. Concentration of each cell lysate was increased on the slides to approximately 2 mg/ml, which was the concentration where there were approximately 600 molecules of well-separated single molecules observable on the 256x512 pixel channel on an Andor EMCCD camera.

After capturing images, each molecule's intensity was drawn into a histogram and then fitted with two Gaussians with a fixed center, where single and double EGFP intensity should be. To verify that each Gaussian actually represented monomer and dimer populations, we also analyzed the proposed monomer and dimer populations by bleaching the molecules and counting the number of bleaching steps. Bleaching steps were counted automatically using a program that finds the number of steps within the bleaching traces of EGFP. Briefly, the program uses the following algorithm:

1. Intensity traces longer than 1 min (enough time for EGFP to be bleached) of selected regions of interest (ROI) with EGFP molecules are drawn.
2. Intensity traces are then smoothed into a step-wise function using the Kalafut-Visscher algorithm.
3. Minimum step heights are determined by control EGFP bleaching experiments are manually set as a user defined variable and used as a threshold.
4. Finally, any step heights of the intensity traces above the threshold are counted.

SNAP-EGFR-EGFP clusters (oligomers larger than a monomer or dimer), which were only observed in the EGF-biotin treated sample, were too bright to completely bleach and quantify for exact receptor number using the bleaching step algorithm. To estimate the number of SNAP-EGFR-EGFP molecules in the clusters, we measured and graphed the pixel intensities of all the regions of interest on the image, which included monomers, dimers, and clusters. The intensities were graphed as a histogram and the intensity of single EGFP was calculated as the population of pixels with the lowest peak intensity level. The SNAP-EGFR-EGFP dimer population was identified as being twice the intensity level as the monomer. And finally, the cluster population's mean intensity was divided by mean value of single EGFP to estimate the number of SNAP-EGFR-EGFP molecules in the cluster.

SUPPLEMENTAL REFERENCES

Eichel, K., Jullié, D., Zastrow, von, M., 2016. β-Arrestin drives MAP kinase signalling from clathrin-coated structures after GPCR dissociation. Nat Cell Biol 18, 303–310. doi:10.1038/ncb3307

Hsiao, S.C., Shum, B.J., Onoe, H., Douglas, E.S., Gartner, Z.J., Mathies, R.A., Bertozzi, C.R., Francis, M.B., 2009. Direct cell surface modification with DNA for the capture of primary cells and the investigation of myotube formation on defined patterns. Langmuir 25, 6985–6991. doi:10.1021/la900150n

Jain, A., Liu, R., Ramani, B., Arauz, E., Ishitsuka, Y., Ragunathan, K., Park, J., Chen, J., Xiang, Y.K., Ha, T., 2011. Probing cellular protein complexes using single-molecule pull-down. Nature 473, 484–488. doi:10.1038/nature10016